Chapter 3

Self-assembled Nanofibers of

Polycyclic Aromatic Hydrocarbon

Polycyclic aromatic hydrocarbon molecules possessed electron-rich central core, which contributes great dispersion force to assemble planar molecules into columnar. In this chapter, coronene, consisting of seven peri-fused benzene rings, was used to form 1D nanostructures. Nanofibers with diameter ca. 66nm have been synthesized from coronene by low temperature (~45 ºC) vacuum sublimation without the aid of catalyst. This polycyclic aromatic hydrocarbon-carbon nanofibers (PAH-CNFs) reveal much better thermal stability than commercial carbon nanotubes (CNTs) and exhibit field emission characteristics with the onset electric field 5.4 V/μm and field enhancement factor 1326 cm^{-1} for 100 μm interelectrode distance. The relative high thermal stability and easier process open a possibility to fabricate large-scale field emission devices in an efficient way and provide a broad range of applications in nanoscience and technology.

3.1 Introduction

Recently, one-dimensional (1-D) carbonaceous nanostructures such as tubes, fibers, wires and rods have become the focus of intensive research owing to their unique applications in nanoscale devices. For example, carbon nanotubes (CNTs) could act as tips of scanning probe microscope [106], field emitters in flat panel displays [107], single-molecular transistors [108], quantum wires [109], and electron emitters for generating x-rays [110].

Various methods to synthesize 1-D carbonaceous nanostructures have been brought up by many research groups. Arc discharge [111], laser ablation [112], pyrolysis [113] and catalytic decomposition of hydrocarbons [114] were common methods to produce CNTs or carbon nanofibers (CNFs). Both the arc and laser ablation were inadequate on the point of view of large-scale production. The catalytic decomposition method has seemed to be the most promising one at present owing to the cheaper investment and lower reaction temperature (650 ºC).

To date, the lowest temperature to fabricate CNTs through the catalytic decomposition method was about 400 ºC on the assistance of plasma enhanced chemical vapor deposition (PECVD) with Ni alloy as catalyst [68]. However, the expensive equipment and confined deposition area limited by electrode size made this process still hard to scale-up.

According to the discussion in chapter 2, planar molecules can self-assemble to form 1D nanostructures under a delicate balance of intermolecular and interfacial forces. In this chapter, coronene, one of the polycyclic aromatic hydrocarbon molecules, was studied to evaluate the feasibility of forming carbonaceous nanofibers in a much lower temperature, which mainly utilizes the π–π interaction to stack planar molecules in one direction [115]. In order to find out the crucial factors that influence the film morphology, various factors, i.e., deposition time, deposition rate, substrate temperature, and surface energy, were taken into account.

3.2 Experimental Section

Using coronene ($C_{24}H_{12}$; Acros), one kind of PAH molecules as starting material, PAH-CNFs were fabricated on a gold substrate by vacuum sublimating coronene from a heated crucible (~45 ºC) in a deposition rate of ~6 Å/min. The gold substrate was kept at room temperature and the background pressure around 3×10^{-6} Torr. Structural investigations were carried out in a Joel JSM-6500F scanning electron microscope (SEM). Contact angles and surface free energies were determined using a KRŰSS universal surface tester (model GH-100). Thermal stability was evaluated by Hitachi thermal desorption system – atmospheric pressure ionization mass spectrometer (TDS-APIMS).

3.3 Results and Discussion

Figures 3-1 (a) and (b) show SEM images of PAH-CNFs deposited by vacuum sublimation with a deposition rate of 6 Å/min for 90 minutes. The fibers were nearly vertically grown on gold substrate with a uniform average density of 10^8 /cm^2, which is slightly less than that of CNTs synthesized by Ni-catalyzed PECVD process (~10^9 /cm^2) [116]. Calculating from several similar SEM images as Figure 3-1 (b), the tip radius, diameter, and length histograms were plotted as shown in Figures 3-2 (a), (b) and (c). The tip radius was determined by placing an approximate circle on each fiber tip then measured radius of each circle. The tip radius, which characterizes the field emission, ranged from 10 nm to 50 nm and the mean value was 30 nm. The mean diameter calculated from the histogram was around 66 nm. The fiber lengths ranged from 0.2 μm to 1 μm and the mean length was about 483 nm.

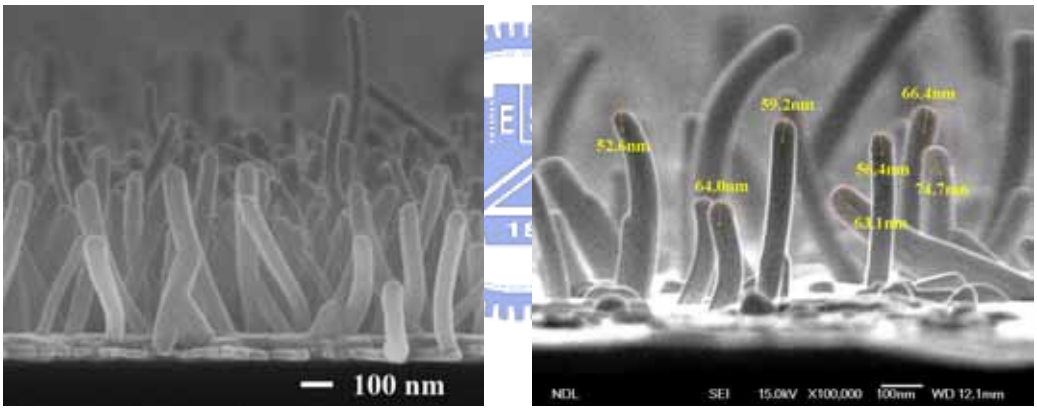

Figure 3-1*(a) Cross-sectional SEM image of PAH-CNFs deposited by vacuum sublimation for 90 minutes. (b) Illustration of the way to caculated the features of PAH-CNFs.*

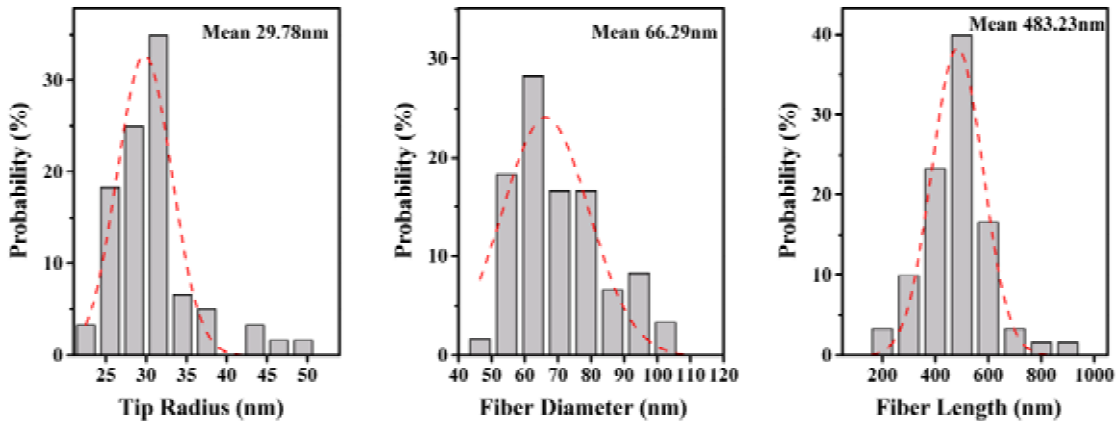

Figure 3-2 *Histograms of (a) tip radius, (b) fiber diameter and (c) fiber length of PAH-CNFs.*

3.3.1 Factors that influence film morphology

The growth mechanism was different from catalytic decomposition method that normally involves three steps: (i) decomposition of hydrocarbon reactants on catalyst surface; (ii) forming a supersaturated solution of carbon and catalyst; and (iii) precipitation of carbon which extrudes the walls [117, 118]. Neither usage of catalyst nor heating substrate in this approach, growth of PAH-CNFs seems having nothing to do with decomposition and rearrangement of coronene.

For aromatic hydrocarbons, which possess large polarizabilities and small local dipole moments, the dispersion interaction would attract molecules to stack in column [115, 15]. However, the repulsive force among nuclei may lead to a parallel-displaced conformation resulting in a tilted columnar structure [15]. The same situation was found in Figures 3-1, the fiber growing direction was nearly vertically aligned but slightly tilted in an angle of 5 ~ 10° away from verticality.

To figure out the factors that influence the film morphology, various issues, i.e., deposition time, deposition rate, substrate temperature, and surface energy, were discussed as follow:

3.3.1.1 Deposition time

Figures 3-3 (a)-(c) show the change of fiber length was a function of deposition time. At the beginning of film deposition, coronene molecules preferred to nucleate separately on the gold substrate as shown in Figure 3-3 (a). Some are small spheres, while others formed pillar structures with a diameter of ca 60 nm, and a length of ca 150 nm. As the deposition time increased, instead of spreading out to form a continuous film, these pillars grow to form high-aspect-ratio fibers. This phenomenon implies that coronene molecules have a greater intermolecular force than the interfacial force.

Figure 3-4 (a) shows a rice paddy-like morphology of CNFs, which were fabricated with longer deposition time. As the deposition time extended, the coming adsorbates not only deposit on those pillared structures, but also on the region among fibers, as shown in Figure 3-4 (b). Consequently, the density of fibers increases with deposition time. Noteworthily, those adsorbates deposited among nanofibers, do not develop to form 1D nanostructures. It might due to the geometry shielding effect resulted from neighboring

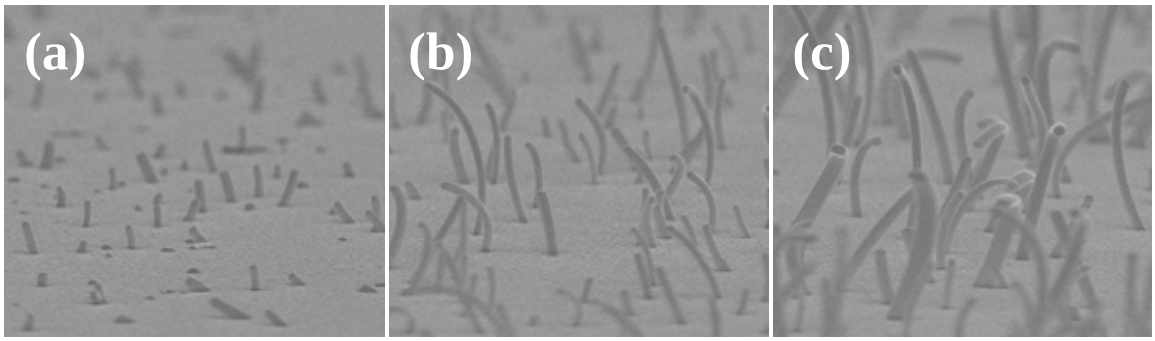

Figure 3-3 *SEM images of PAH-CNFs deposited by vacuum sublimation for (a) 1 minute, (b) 2 minutes, and (c) 15 minutes, respectively.*

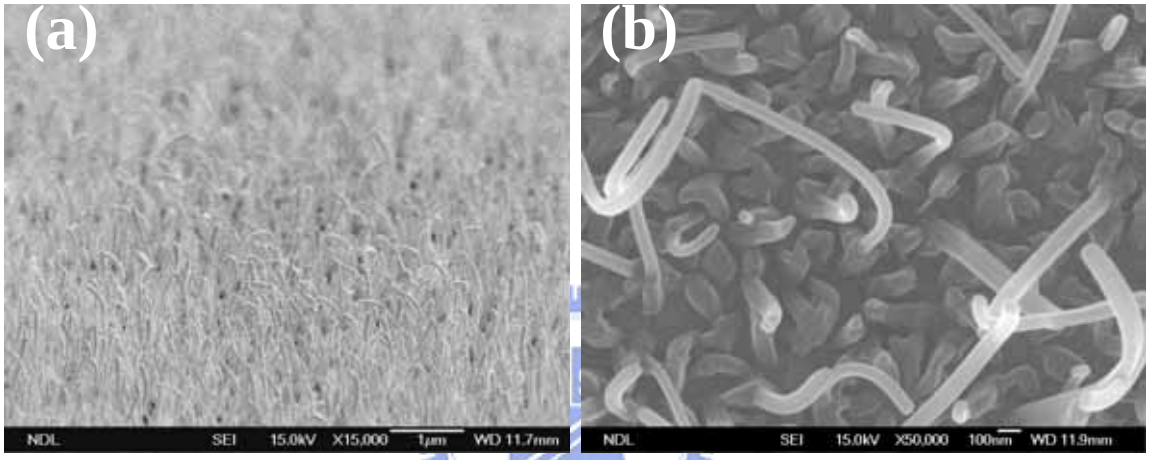

Figure 3-4 *(a) Side-view SEM images and (b) top-view SEM images of PAH-CNFs deposited by vacuum sublimation for 120 minutes.*

long fibers that block the mass transfer of coronene, hence alter the morphology.

3.3.1.2 Deposition rate

Figures 3-5 (a) and (b) present the side-view SEM images of PAH-CNFs deposited with rates of 0.1 Å/sec and 8 Å/sec, respectively. No significant differences were observed in fiber density and fiber length. It might be owing to the large dimension of our deposition chamber that cause a longer diffuse path (~ 35 cm) for coronene molecules to fly from the crucible to the substrate, hence the substrate does not experience much different in the concentration of coming adsorbates. However, as I place the gold substrate right above the crucible at a distance of 3 cm, a very thick film consisted of numerous entangled fibers was observed. Consequently, I believe the fibers can grow much longer and densely with a higher deposition rate.

Additionally, with a constant deposition rate, if I rotate the substrate with a rotor, the

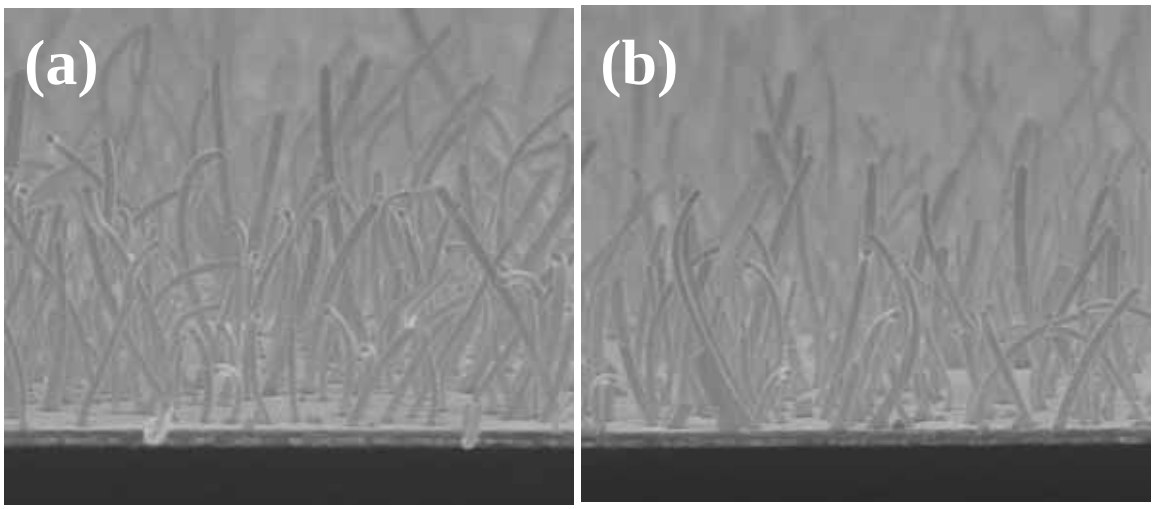

Figure 3-5 *Side-view SEM images of PAH-CNFs deposited on gold substrate with rates of (a) 0.1 Å/sec and (b) 8 Å/sec.*

high angular speed will cause the fibers grow aslant. Owing to adsorbates need time to diffuse to energy-favored sites; substrate rotation will prohibit those coming adsorbates from stacking up perfectly.

3.3.1.3 Substrate Temperature

Figures 3-6 (a) – (c) show the side-view SEM images of PAH-CNFs deposited at 40 °C, 60 °C and 100 °C, respectively. These figures reveal that fiber length decrease with temperature. At high substrate temperature, parts of adsorbates desorb from the substrate, hence finite reactant were available to stack up as long fibers. Noteworthily, these organic fibers can endure high temperature without decomposing under vacuum condition reveals a great thermal stability, which will be further examined by a thermal desorption spectrometer (TDS).

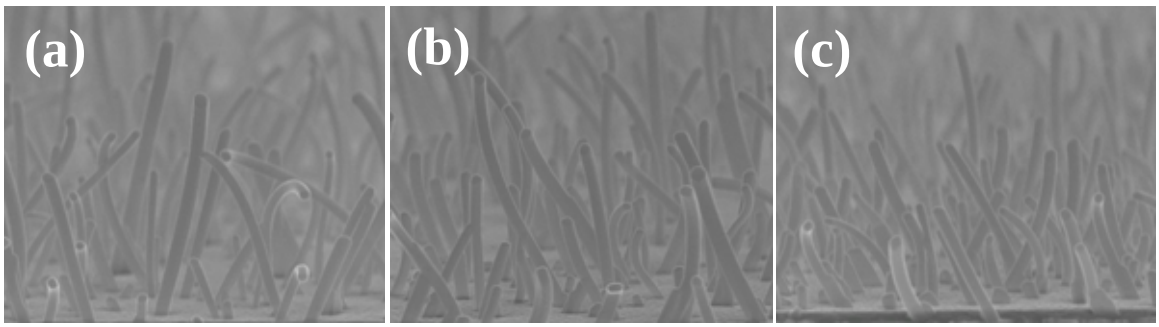

Figure 3-6 *Side-view SEM images of PAH-CNFs deposited at (a) 40 ℃, (b) 60 ℃ and (c) 100 ℃, respectively.*

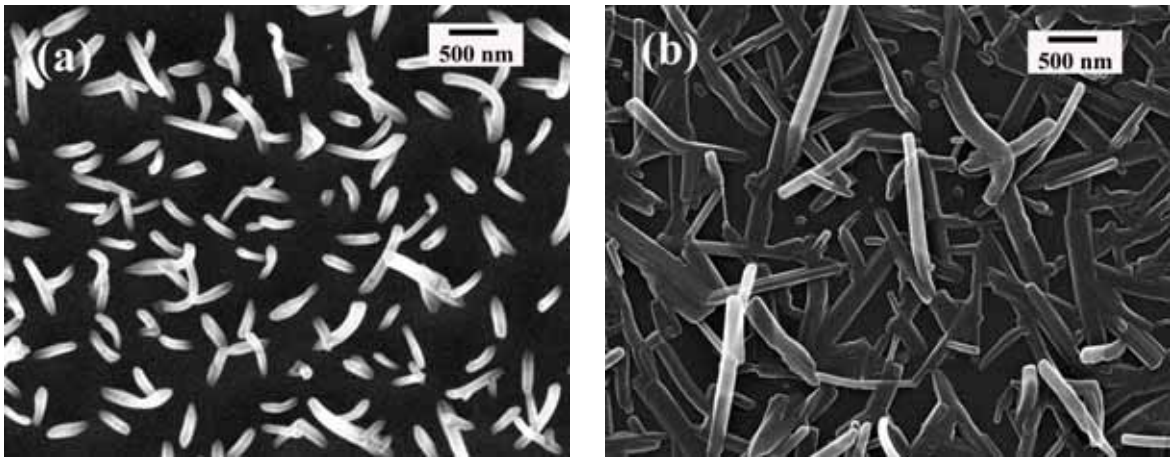

Figure 3-7 *Top-view SEM images of PAH-CNFs deposited on (a) gold substrate and (b) silicon dioxide substrate.*

3.3.1.4 Substrate Effect (Surface Energy)

Besides the dispersion force, the surface energy of substrate, which relates to the unsaturated surface bond, also affects the geometry of PAH-CNFs. Figure 3-7 shows top-view SEM images of PAH-CNFs on (a) gold substrate and (b) silicon dioxide substrate. The fibers on gold substrate stood up straightly, however those on silicon dioxide surface lay down and entangled in the majority. The better wettability of silicon dioxide might due to the higher concentration of unsaturated surface bonds, which tend to adsorb molecules to lower the surface free energy. This is consistent with our results on contact angle measurement. The surface free energy was 40 mJ/m^2 for gold substrate and 49 mJ/m^2 for silicon dioxide substrate. These values were calculated by Owens method from the measured contact angles for three different solvents (diiodo methane, ethylene glycol and water) on each substrate. As coronene molecules deposit on silicon dioxide, the π–π interaction still holds discotic molecules together, however the existing of π-surface bonds results in an edge-on morphology rather than a face-on morphology [119].

3.3.2 HRTEM

Figures 3-8 (a) presents the HRTEM image of the single PAH-CNF, with a diameter of 51 nm. Unlike in the case of CNTs, no catalyst was observed at the top of the fiber. This finding was further verified by the energy dispersive spectra (EDS), no gold signal was observed along the length of the fiber. Figure 3-8 (b) magnifies the image of this nanofiber and reveals indistinctly that coronene molecules stacked in the growth direction and parallel to each other. This high-resolution image indicates that the PAH-CNFs are

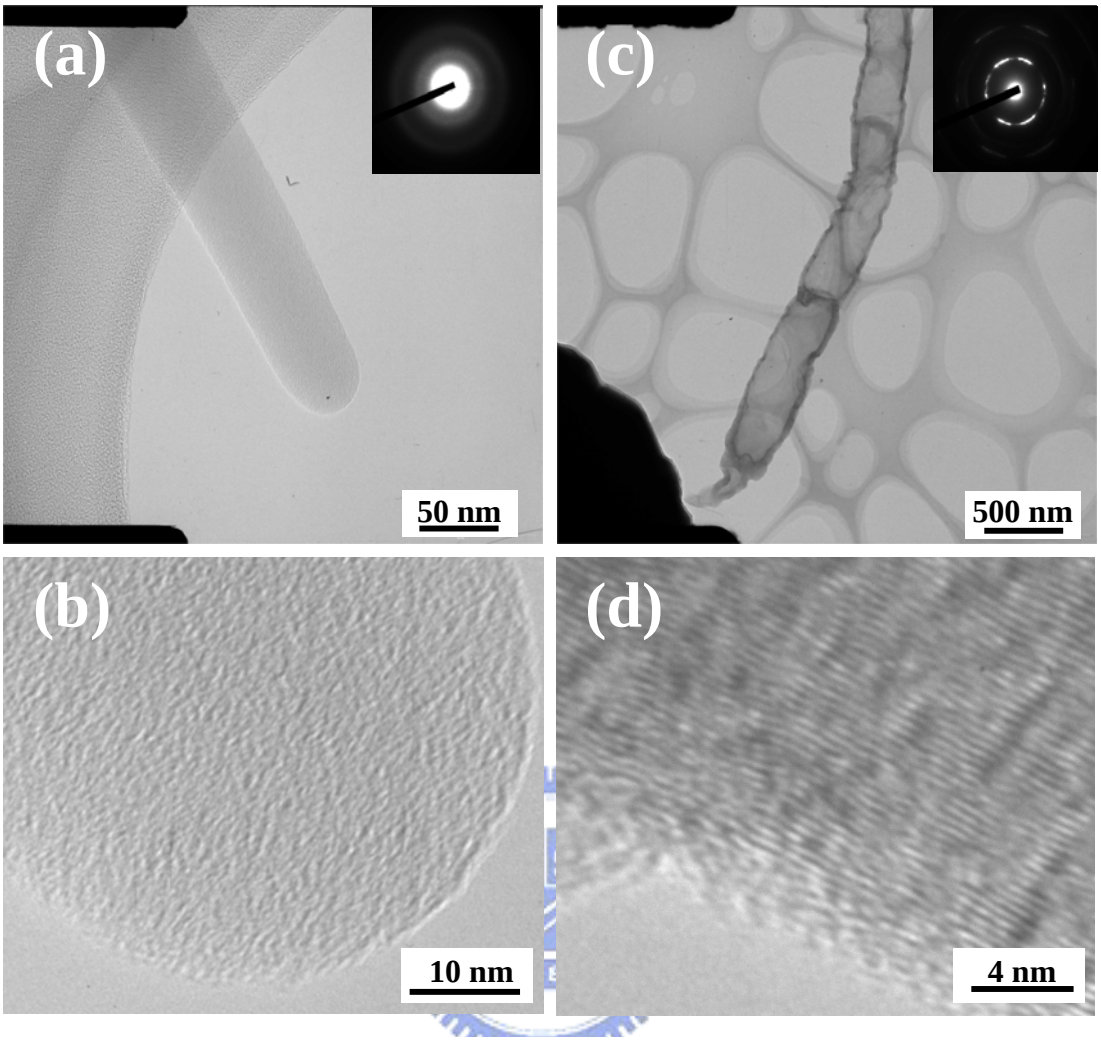

Figure 3-8 *(a) HRTEM image of a single PAH-CNF (diameter: 51 nm). Inset: the corresponding electron diffraction pattern. (b) Magnified image of this nanofiber. (c) HRTEM image of a hollow PAH-CNF (diameter: 420 nm). Inset: the corresponding electron diffraction pattern. (d) Magnified image of this hollow nanofiber along the edge.*

formed by stacking coronene molecules layer upon layer. However, the electron diffraction pattern presented in the inset of Figure 3-8 (a) displays only amorphous rings, rather than distinct diffractive spots, suggesting an insignificant degree of crystallinity.

Besides the core-filled nanofiber structure, interestingly, I also observed certain 1D hollow structures in HRTEM analysis. Figure 3-8 (c) shows the TEM images of a wider-diameter (~420 nm), longer-length and jointed hollow-structure. Figure 3-9 (d) magnified this structure at the edge side, and parallel fringes were observed distinctly. The average interlayer distance determined using Fuji Imagegauge software was 3.4 Å, a standard value of graphite. When selected area diffraction (SAD) was performed, a clear

diffraction pattern was observed, as shown in the inset of Figure 3-8 (c). The mechanism of forming this hollow-structure is not clear, but Jiang et al. has reported a way to synthesis multiwall CNTs, which is mainly utilizing benzene as precursor, and coronene derivatives as intermediate products to form the bamboo-like CNTs [120]. I believe that a similar mechanism were involved in both case.

3.3.3 Thermal Stability

Thermal stability is a crucial property to evaluate feasibility for applying a new material in use. TDS-APIMS was used here to monitor thermal desorption behavior of PAH-CNFs by heating the sample from 25 °C up to 800 °C at a ramp rate of 10 °C/min. For comparison, the same area size CNTs film deposited by electrophoresis [121] was measured in the same condition. Figure 3-9 (a) shows the CO_2 (m/z = 44) desorption curve of both PAH-CNFs and CNTs and it reveals that PAH-CNFs are very stable for less carbonaceous species are oxidized and desorbed as CO_2 for PAH-CNFs than for CNTs. The better thermal stability of PAH-CNFs can be further confirmed by much less desorption of benzene species C_6H_6 (m/z = 78) as shown in Figure 3-9 (b). The superior thermal stability might attribute to the chemically perfect π-delocalization in these seven aromatic rings of coronene, which consequently offers stronger C-C bonds. Despite that CNTs possess the similar structure, the unexpected structural defect arose during synthesis, e.g. saturated C-C bond or open rings, will degrade the structural stability. Besides, the amorphous porous carbon congested among the tubes or the residues from electrophoresis

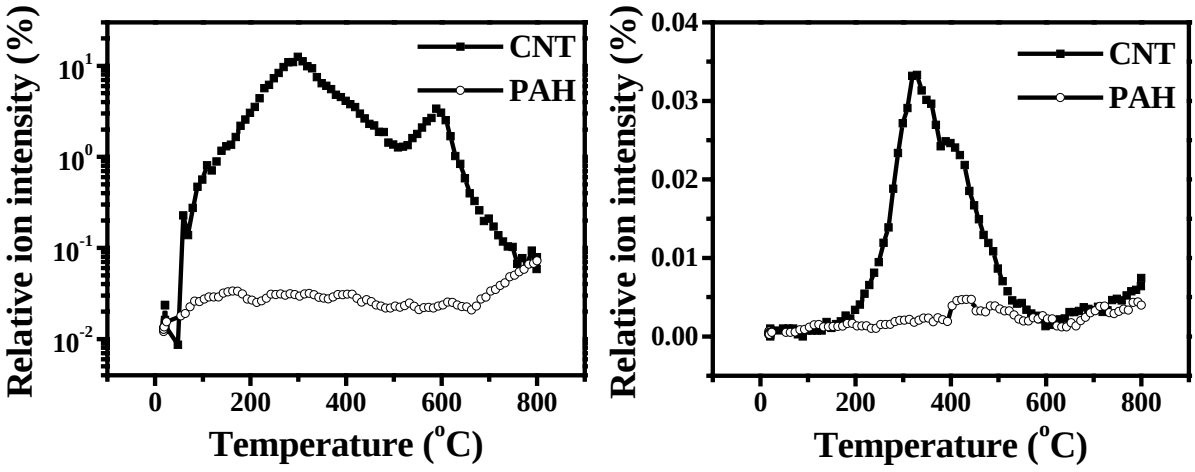

Figure 3-9 *Thermal desorption curve of (a) CO_2 (m/z = 44) and (b) C_6H_6 (m/z = 78) for both CNTs and PAH-CNFs.*

process also result in the larger desorption of CO_2 for CNTs [122]. The thermal decomposition occurred above 600 °C of PAH-CNFs was similar with the results of other reports for CNTs [114, 122, 123].

3.3.4 Field Emission of CNFs film

Field emission of PAH-CNFs was measured by placing a cylindrical electrode of 2.2 mm diameter above the fibers surface at a distance of 100 μm. All the measurements were carried out in a vacuum chamber under a pressure of 10^{-6} Torr with Keithley 237 as a power supplier and a current meter. Figure 3-10 shows a typical plot of the emission current density *J* versus the applied field *E*. The onset field for producing a current density of 10 μA/cm^2 was near 5.4 V/μm. This result is similar with CNTs array (~5.5 V/μm) that measured with the same method [124]. The inset in Figure 3-10 reveals *J-E* characteristics for PAH-CNFs followed Fowler Nordheim (FN) behavior. After a well-defined FN type threshold field, there is an exponential current rise region, followed by saturation. This saturation occurred at high voltage might result from the deficiency of emitting electrons that happened owing to the burning out of emitting tips [125] or the saturate drift velocity of carriers in the fibers [126]. Because PAH-CNFs were

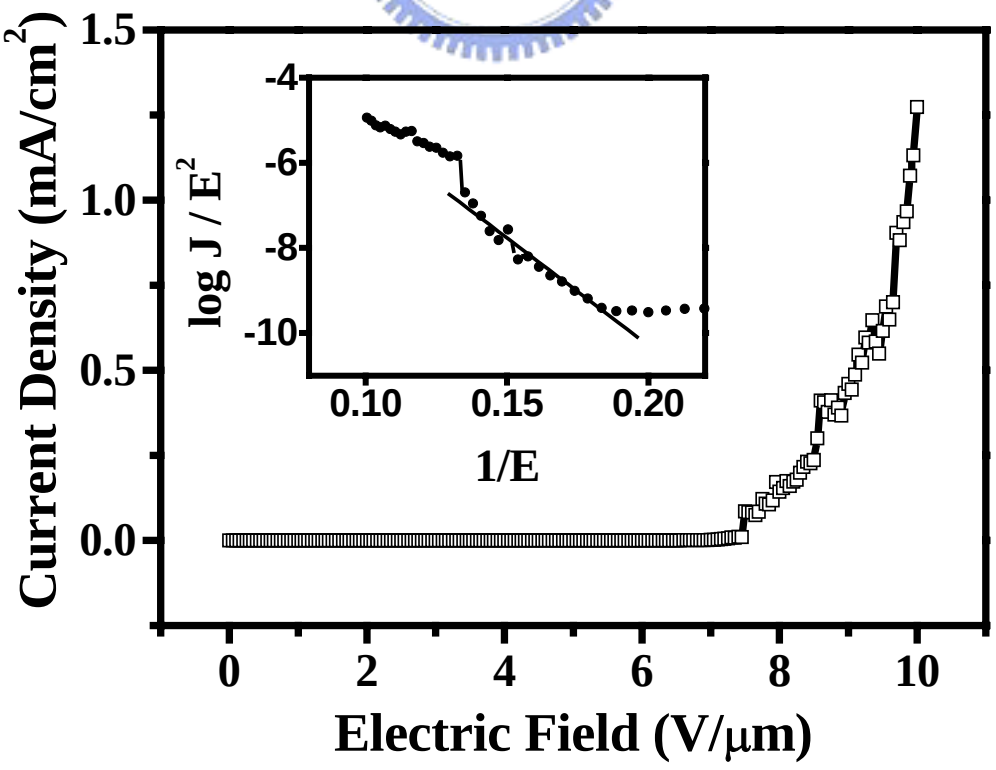

Figure 3-10 *J-E curve of PAH-CNFs. Inset: corresponding Fowler-Nordheim plot.*

constructed by superposing PAH molecules on each, the electrons were transported across molecules under the bias of electric field. Normally, intermolecular transporting is slower than intramolecular transporting, so the limited drift velocity might be the reason of current saturation.

The field enhancement factor β is defined as $\beta = F/E$, where F is effective electric field at the surface of tip and E is the applied electric field. Taking the tip work function to be that of graphite (~ 5eV) as most case of CNTs [127], the field enhancement factor β could be deduced from the slope of fitting line, which was approximately 1326 cm^{-1}, analogous to the value of CNTs film (1000 ~ 3000 for 125 μm interelectrode distance) [127]. Normally, β is inversely proportional to the tip radius in the concept of electrostatic properties [128]. The lager radius of PAH-CNFs (~30 nm), as compared with MWNT tip (~4 nm) [129], resulted in a smaller β value that caused the higher onset electric field. Moreover, I observed the longer PAH-CNFs needed higher electric field to produce the same current density of the shorter one. The certain resistance raised from the slower intermolecular electron transporting might be responsible to the higher onset electric field.Figure 3-11 displays the emission current stability of the PAH-CNFs film

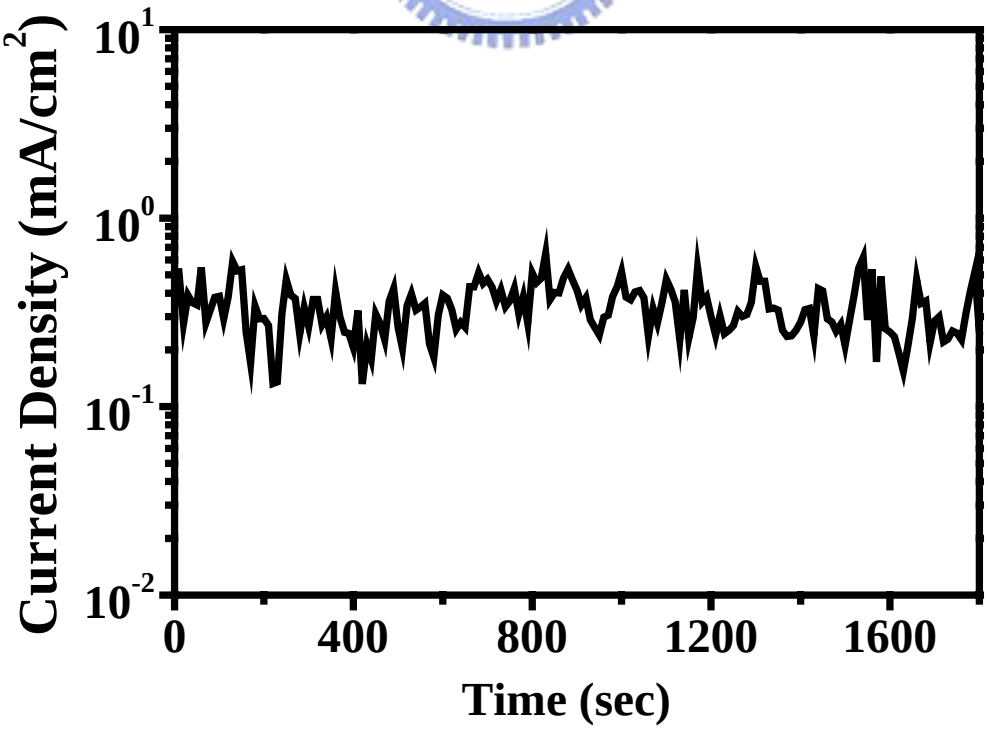

Figure 3-11 *Emission current stability of the PAH-CNFs at constant voltage.*

when biased at 900 V (E = 9 V/μm) for 1800 s. The mean current density was ca. 0.4 mA/cm^2 with a perturbation of less than one order of magnitude. The field emission current did not decay during the stability measurements, demonstrating that the PAH-CNFs film is suitable for applications as electron emitting devices.

3.3.5 Field Emission of single individual CNF

In order to make sure that the current I measured in vacuum is indeed resulted from the PAH-CNFs; a tungsten probe moved by a step motor was assembled to the SEM instrument. By approaching the probe toward the nanofiber with accuracy of nanometer scale, I can measure the field emission current of single nanofiber within a precise distance. Figure 3-12 present the SEM image of a tungsten probe kept at a distance of 200 nm above a one-micrometer-long PAH-CNF. Owing to the tip radius of tungsten probe is around 145 nm, a value that is smaller than the space between two individual fibers, I can evaluate the field emission characteristic of single individual CNF without the interference of electrostatic shielding effect caused by other neighboring fibers.

Figure 3-13 plots the field emission performance of the single individual PAH-CNF, which was shown in Figure 3-12. The turning point of the curve for producing a current of 1 nA was near 205 V. This value is higher than the result of CNTs, i.e. 115 V measured by keeping anode at a distance of 1.25 μm [130]. As compared with

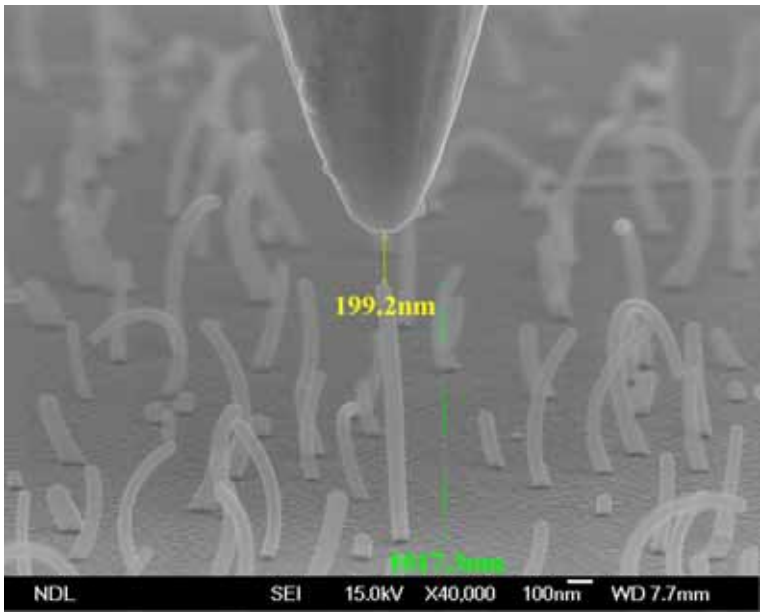

Figure 3-12 *SEM image of a tungsten probe kept at a distance of 200 nm above a one-micrometer -long PAH-CNF.*

previous result of PAH-CNFs film, for emitting 0.4 mA/cm^2 current from 10^8 fibers needs an electric field of 9 V/μm. Under this circumstance, each fiber donates 4 fA current, which is deduced from an easy calculation. In the single fiber emission experiment, 1 nA current was extracted under an electric field of 1025 V/μm (205 Volt operated at a distance of 200 nm). This field is about 114 times higher than the value of film structure. But as far as the emission current was concern, single individual fiber emits 250 times higher current than the fiber that mounted among multi-fibers film (1 nA vs. 4 fA). This result means that not all of the fibers contribute to emit electron when the emission current was collected form a PAH-CNFs film. The similar phenomenon was observed and discussed by Bonard el al. for CNTs film; the electrostatic shielding effect might be the reason [101]. Besides, the longer distance between the anode and the fibers for CNTs film system, electrons might emit at any angle, consequently, finite current was measured. The inset in Figure 3-13 reveals *J-E* characteristics for PAH-CNFs followed Fowler Nordheim (FN) behavior. The conductance spike is due to that PAH-CNFs were constructed by superposing PAH molecules on each; the electrons were transported across molecules under the bias of electric field. Normally, intermolecular transporting is slower than intramolecular transporting, so the limited drift velocity might be the reason of current perturbation [131].

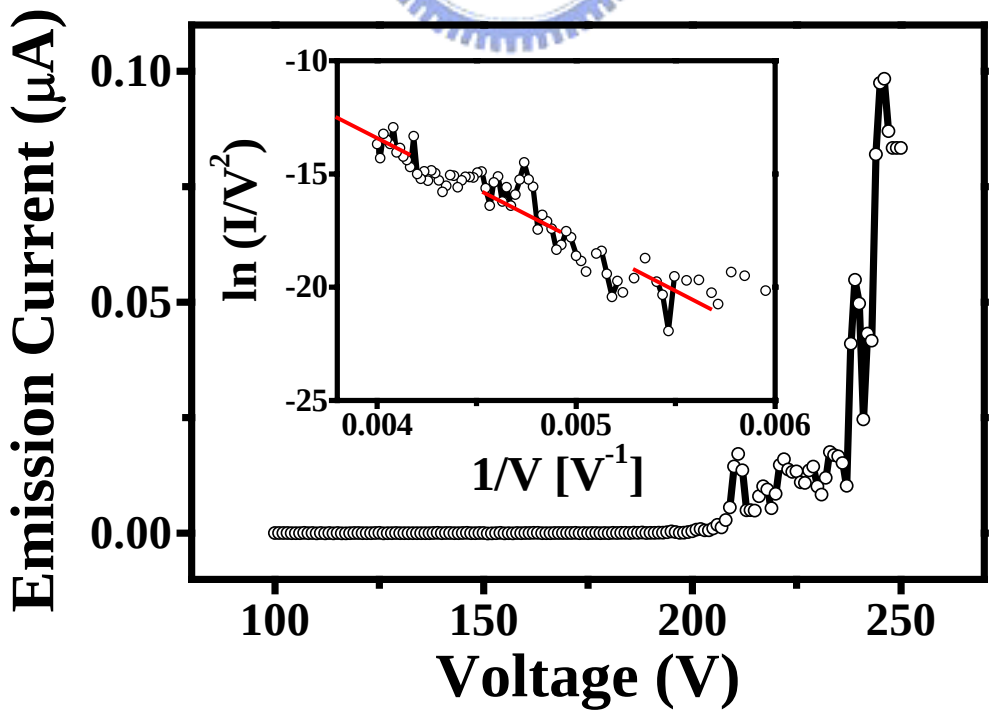

Figure 3-13 *The field emission performance of the single individual PAH-CNF. The inset reveals J-E characteristics for PAH-CNFs followed Fowler Nordheim behavior.*

3.3.6 Application as a pillar template

The high aspect ratio morphology of PAH-CNFs can be utilized not only as a field emitter, but also as a template to form a rougher surface for certain film. By this way, film property might be altered from hydrophile to hydrophobe with similar effect as the well-known lotus effect [86]. It is important for those applications on micro fluid channel that the channel walls need to be hydrophobic in order to reduce the interaction between the fluid and the channel wall. Moreover, various lengths of PAH-CNFs will affect the field emission characteristic. To obtain fibers with uniform length, chemical mechanical polishing (CMP) was introduced to remove the excess fiber length [132]. However, the accompanied huge shear stress will peel off the fibers. Hence a robust film has to be deposited first to protect and solidify those fibers on the gold substrate. After the trim of fiber length by CMP, the capped film can be removed by wet chemical process easily.

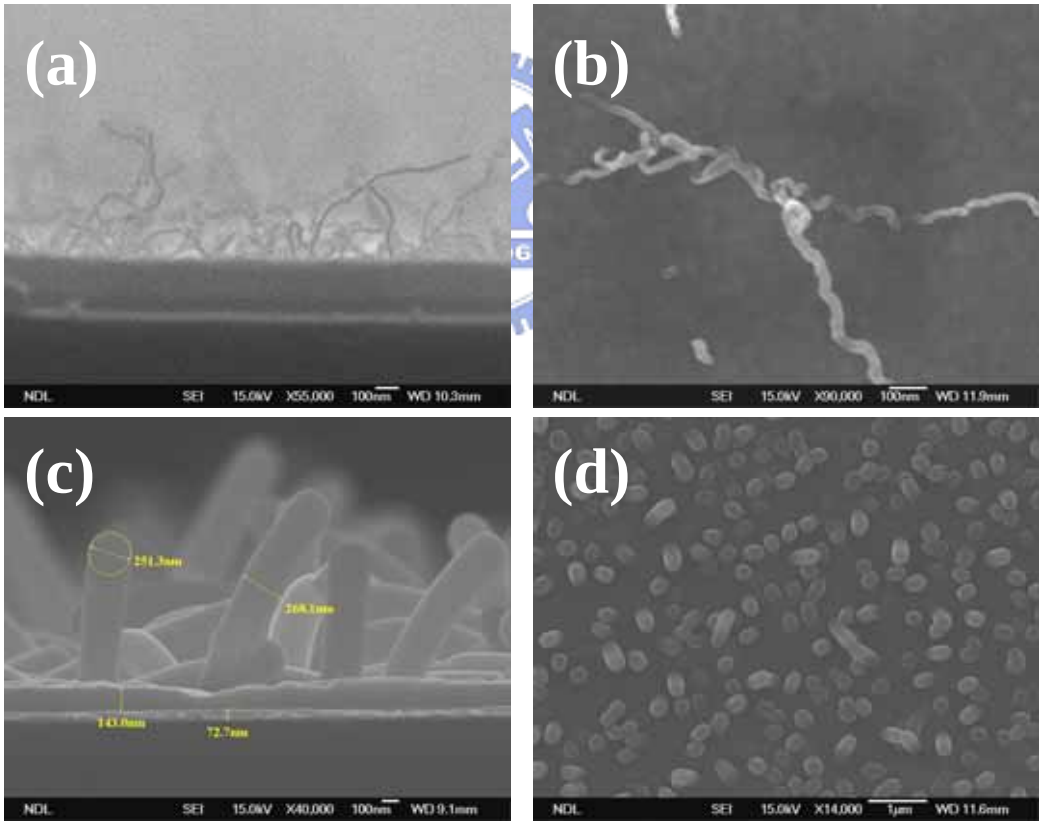

Figure 3-14 *(a) side-view and (b) top-view SEM images of PAH-CNFs capped with silicon dioxide by PECVD process. (c) side-view and (d) top-view SEM images of PAH-CNFs capped with silicon nitride by PECVD process.*

Based on these two concepts, I deposit both silicon dioxide and silicon nitride on the PAH-CNFs film with PECVD process (300 °C and 300 mTorr). Figure 3-14 (a) and (b) show the side- and top-view SEM images of PAH-CNFs film, which were capped with a thin silicon dioxide layer. Owing to oxygen was involved in the SiO_2 PECVD process; these organic fibers were easily oxidized and cannot survive under this condition. Consequently, the PAH-CNFs turns to be thinner and twisty. However, if I deposited silicon nitride on PAH-CNFs, due to nitrogen reactant is inert to coronene molecules, a thick and straight pillar morphology was obtained [Figures 3-14 (c) and (d)]. The diameter of 1D nanostructure was changed from 66 nm to 265 nm, and the fiber length was still kept the same as the original fibers. Noteworthily, the PECVD process was performed in a vacuum chamber with temperature of 300 °C, this result demonstrated its good thermal stability and was consistent with the results of TDS.

3.4 Conclusions

In summary, by utilizing coronene as starting material, carbon nanofibers were deposited simply by low temperature (~45°C) vacuum evaporation without the help of catalyst and high temperature. The nearly vertical growing PAH-CNFs on gold substrate was dominated by π-π interaction and surface energy. This PAH-CNFs reveal much better thermal stability than commercial CNTs. They also exhibit field emission characteristics and follow Fowler Nordheim behavior as the CNTs. The higher turn-on field of PAH-CNFs than that of the CNTs for electron emission is owing to that the intermolecular charge transfer is slower than the intramolecular charge transfer. The CNTs resemble a rolled-up graphite, and the electron transport is mainly within the same sheet, which possesses a better conductivity. However, the electron conduction of PAH-CNFs is mainly through hopping among different molecular planes, hence a higher driving voltage is needed to emit a comparable current. Nevertheless, the relative high thermal stability and easier process still provide a broad range of applications in nanoscience and technology.